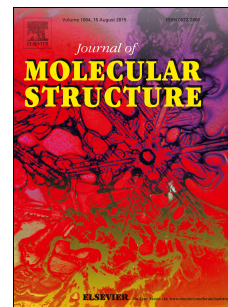


Journal Pre-proof

Synthesis, cytotoxic activity and quantum chemical calculations of new 7-thioxopyrazolo[1,5-f]pyrimidin-2-one derivatives

Zülbiye Kökbudak, Murat Saracoglu, Senem Akkoç, Zeynep Çimen, M. Izzettin Yilmazer, Fatma Kandemirli



PII: S0022-2860(19)31370-5

DOI: <https://doi.org/10.1016/j.molstruc.2019.127261>

Reference: MOLSTR 127261

To appear in: *Journal of Molecular Structure*

Received Date: 13 June 2019

Revised Date: 18 October 2019

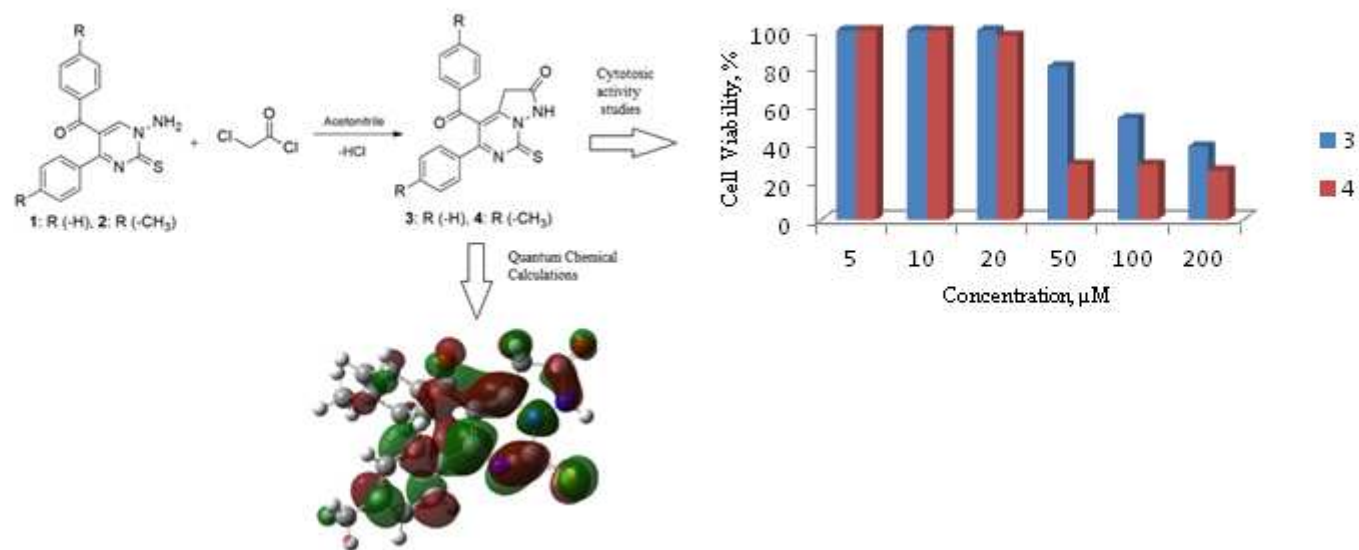
Accepted Date: 19 October 2019

Please cite this article as: Zü. Kökbudak, M. Saracoglu, S. Akkoç, Z. Çimen, M.I. Yilmazer, F. Kandemirli, Synthesis, cytotoxic activity and quantum chemical calculations of new 7-thioxopyrazolo[1,5-f]pyrimidin-2-one derivatives, *Journal of Molecular Structure* (2019), doi: <https://doi.org/10.1016/j.molstruc.2019.127261>.

This is a PDF file of an article that has undergone enhancements after acceptance, such as the addition of a cover page and metadata, and formatting for readability, but it is not yet the definitive version of record. This version will undergo additional copyediting, typesetting and review before it is published in its final form, but we are providing this version to give early visibility of the article. Please note that, during the production process, errors may be discovered which could affect the content, and all legal disclaimers that apply to the journal pertain.

© 2019 Published by Elsevier B.V.

Graphical Abstract:



Synthesis, cytotoxic activity and quantum chemical calculations of new 7-thioxopyrazolo[1,5-f]pyrimidin-2-one derivatives

Zülbiye Kökbudak ^{1*}, Murat Saracoglu ², Senem Akkoç ³, Zeynep Çimen ⁴, M. Izzettin Yilmazer ² and Fatma Kandemirli ⁵

¹ *Erciyes University, Faculty of Science, Department of Chemistry, 38039, Kayseri, Turkey*

² *Erciyes University, Faculty of Education, 38039, Kayseri, Turkey*

³ *Suleyman Demirel University, Faculty of Pharmacy, Department of Basic Pharmaceutical Sciences, 32260, Isparta, Turkey*

⁴ *Ankara Hacı Bayram Veli University, Polatlı Faculty of Science and Arts, Department of Chemistry, 06900, Ankara, Turkey*

⁵ *Kastamonu University, Faculty of Engineering and Architecture, 37150, Kastamonu, Turkey*

*Corresponding author: E-mail: zulbiye@erciyes.edu.tr (Z. Kökbudak)

ABSTRACT

The reactions of 1-amino-2-thioxo-1,2-dihydropyrimidin derivatives **1** and **2** with chloroacetyl chloride in the presence of sodium acetate led to the formation of 7-thioxopyrazolo[1,5-f]pyrimidin-2(1*H*,3*H*,7*H*)-one derivatives (**3** and **4**) in 78-80% yields. The structure of these newly synthesized compounds **3** and **4** were fully characterized by ¹H NMR, ¹³C NMR, FT-IR spectroscopies and elemental analyses. The quantum-chemical calculations were made to find molecular properties of the **3** and **4** by using DFT/B3LYP method with 6-311++G(2d,2p) basis set. Quantum chemical features such as HOMO, LUMO, energy gap, ionization potential, chemical hardness, softness, electronegativity, dipole moment and etc. values for gas and solvent phase of neutral molecules were calculated and discussed. Furthermore, the cytotoxic activities of **3** and **4** were tested against human liver cancerous cell line (HepG2) and human breast cancerous cell line (MDA-MB-231) for 24 h and 48 h, respectively.

Keywords: Cytotoxic activity; DFT; Pyrimidine; Quantum chemical calculations.

1. Introduction

Pyrimidine and its derivatives continue to attract considerable attention due to very wide spectrum of biological activities. Numerous pyrimidine derivatives are reported that they exhibit antifungal [1], antiviral [2], anticancer [3], anti-inflammatory [4] and antihistaminic [5] activities. Some pyrazole such as Celebrex [6], Viagra [7] and Acomplia [8] are commercially available. Similarly, pyrazolopyrimidine derivatives have attracted wide pharmaceutical interest because of their anti-trypanosomal activity [9], anti-schistosomal activity [10], and other activities such as HMG-CoA reductase inhibitors [11], COX-2 selective inhibitors [12].

In recent years, the reactions of 1-amino-2-thioxo-1,2-dihydropyrimidin derivatives with anhydrides [13], 1,3-dicarbonyl compounds [14], acyl chlorides [15,16] and transition metal complexes [17] have been reported. These interesting activities and reactions have simulated chemists to develop the chemistry of this class of compounds.

In the present study, the key starting materials (1-amino-4-phenyl-2-thioxo-1,2-dihydropyrimidin-5-yl)(phenyl)methanone (**1**) and (1-amino-2-thioxo-4-*p*-tolyl-1,2-dihydropyrimidin-5-yl)(*p*-tolyl)methanone (**2**) were prepared in two steps from furan-2,3-diones and acetophenonthiosemicarbazone. These starting materials were reported in earlier published study [19] (**Scheme 1**). After synthesis of **1** and **2**, the new 4-benzoyl-5-phenyl-7-thioxopyrazolo[1,5-*f*]pyrimidin-2(1*H*,3*H*,7*H*)-one (**3**) and 4-(4-methylbenzoyl)-7-thioxo-5-*p*-tolylpyrazolo[1,5-*f*]pyrimidin-2(1*H*,3*H*,7*H*)-one (**4**) were prepared from the reaction of 1-amino-2-thioxo-1,2-dihydropyrimidin derivatives (**1** and **2**) with chloroacetyl chloride (**Scheme 2**). They were characterized by FT-IR, ¹H and ¹³C NMR.

In addition to experimental study, optimization of molecules was performed by using DFT/B3LYP/6-311++G(2d,2p) basis set of Gaussian 09, Revision A.02 program [20]. This basis set is known as one of the basis sets that gives more accurate results in terms of the determination of electronic and geometries properties for a wide range of organic compounds [21]. The quantum chemical calculation of the molecules was carried out using density functional theory/the integral equation formalism polarisable continuum model (DFT/IEFPCM) [22], with basis set 6-311++G(2d,2p) for solvent phase. Quantum chemical parameters of investigated molecules such as the energy of the highest occupied molecular orbital (E_{HOMO}), the energy of the lowest unoccupied molecular orbital (E_{LUMO}), HOMO-LUMO energy gap (ΔE), ionization potential (I), chemical hardness (η), chemical softness

(σ), electronegativity (χ), chemical potential (μ), dipole moment (DM), global electrophilicity (ω) and total of negative MAC, Mulliken charges of some atoms for gas and solvent phase of neutral molecules (**3** and **4**) were calculated, and the relationship between the activity and stability of the molecules of these results was discussed. Recently, the optimization of the molecules with different basic sets by using Gaussian program and the discussion of results have been widely used [18, 23-25].

After completed synthesis and characterization of compounds **3** and **4**, they were tested against two cancerous cell lines for learning their cytotoxic activities.

2. Experimental Section

2.1. General materials and instruments

All necessary solvents and reagents were purchased from Merck and Sigma-Aldrich (Chemicals Pvt Ltd.). Melting points were determined on the digital melting point apparatus (Electrothermal 9100). The synthesized compounds were checked for their homogeneity by TLC. Microanalyses were performed on a Leco CHNSO-932 Elemental Analyser and the results agreed favourably with the calculated values. The IR spectra were recorded on a Shimadzu Model 8400 FT-IR spectrophotometer. Around 3 mg of compounds were put to FT-IR spectrophotometer device and the spectra was taken in a few minutes. The ^1H and ^{13}C NMR spectra were recorded on a Bruker 400(100) MHz Ultra Shield instrument. The chemical shifts are reported in ppm from tetramethylsilane as an internal standard and are given in δ (ppm). A Hitachi UH 5300 Double Beam UV-vis Spectrophotometer (Tokyo, Japan) was used for determining of absorbance values of compounds at 250-800 nm (λ_{max}).

2.1.1. 4-Benzoyl-5-phenyl-7-thioxopyrazolo[1,5-f]pyrimidin-2(1H,3H,7H)-one (**3**)

A mixture of compound **1** (0.2 g, 0.68 mmol), sodium acetate as a base (1g, 12 mmol) and chloroacetyl chloride (0.4 mL, 2.5 mmol) in acetonitrile (50 mL) was stirred with magnetic stirrer at room temperature for 5 h. The solvent was evaporated. Then, the residue was treated with dry diethyl ether. The product **3** which precipitated was filtered off, washed several times with water and recrystallized from ethyl alcohol. Yield: 78%. M.p.: 205-207 °C. Elemental analysis (%) for $\text{C}_{19}\text{H}_{13}\text{N}_3\text{O}_2\text{S}$, Found (Calc.): C= 65.51 (65.69); H= 3.62 (3.77); N= 12.04 (12.10); S= 9.12 (9.23). FT-IR (cm^{-1}) Found (Theo.): 3058 (3210-3172) (aromatic C-H), 2956 (3120-3086) (aliphatic C-H), 1668 (1817) and 1650 (1696) (C=O), 1595-1475

(1603-1533) (C=C and C=N), 1274 (1327) (C=S), 740-660 (820-701) (pyrimidine ring skeleton vib.). ^1H NMR (ppm, found: 400 MHz, CDCl_3), Found (Theo.): 8.53 (10.14) (s, 1H, NH), 7.80-7.28 (8.81-7.45) (m, 10H, Ar-H), 3.62 (4.75-3.79) (s, 2H, CH_2). ^{13}C NMR (ppm, 100 MHz, CDCl_3), Found (Theo.): 190.6, 166.4, 158.7, 156.2, 143.8, 135.0, 134.7, 133.8, 132.2, 130.0, 130.2, 129.6, 129.2, 129.0, 128.2 and 26.5 (201.6, 178.5, 171.3, 170.4, 157.3, 145.6, 144.6, 140.0, 138.1, 137.6, 137.2, 136.8, 136.7, 135.0, 134.9, 133.8, 133.4, 121.6 and 44.2).

2.1.2. 4-(4-Methylbenzoyl)-7-thioxo-5-p-tolylpyrazolo[1,5-f]pyrimidin-2(1H,3H,7H)-one (**4**)

A mixture of compound **2** (0.3 g, 0.89 mmol), sodium acetate as a base (1g, 12 mmol) and chloroacetyl chloride (0.3 mL, 3.76 mmol) in acetonitrile (50 mL) was stirred by a magnetic stirrer at room temperature for 24 h. The solvent was evaporated. Then, the residue was treated with dry diethyl ether. The product **4**, which precipitated, was filtered off and recrystallized from ethyl alcohol. Yield: 80%. M.p.: 214-216 °C. Elemental analysis (%) for $\text{C}_{21}\text{H}_{17}\text{N}_3\text{O}_2\text{S}$, Found (Calc.): C= 66.97 (67.18); H= 4.59 (4.56); N= 11.34 (11.19); S= 8.41 (8.54). FT-IR (cm^{-1}) Found (Theo.): 3066 (3206-3168) (aromatic C-H), 2964 (3114-3112) (aliphatic C-H), 1664 (1815) and 1644 (1637) (C=O), 1595-1569 (1611-1524) (C=C and C=N), 1271 (1328) (C=S), 740-660 (810-717) (pyrimidine ring skeleton vib.). ^1H NMR (ppm, found: 400 MHz, CDCl_3), Found (Theo.): 8.43 (10.14) (s, 1H, NH), 7.72-7.14 (8.67-7.18) (m, 8H, Ar-H), 3.60 (4.73-3.75) (s, 2H, CH_2), 2.42 and 2.33 (2.74-2.19) (s, 6H, 2CH_3). ^{13}C NMR (ppm, 100 MHz, CDCl_3), Found (Theo.): 190.3, 166.7, 158.6, 155.9, 146.5, 143.6, 143.2, 132.3, 131.0, 130.2, 129.9, 129.8, 129.6, 128.1, 26.6, 21.9 and 21.6 (201.0, 178.3, 171.6, 169.4, 156.0, 153.5, 150.8, 142.8, 141.8, 137.8, 136.7, 136.4, 135.6, 135.5, 134.5, 133.9, 122.4, 44.2, 24.1 and 24.0).

2.2. Computational details

Molecular properties, related to the reactivity and selectivity of the compounds, were estimated following the Koopmans's theorem relating the energy of the HOMO and the LUMO. According to the DFT-Koopmans' theorem [26, 27], the ionization potential (I) can be approximated as the negative value of E_{HOMO} , such as shown in equation 1:

$$I = -E_{\text{HOMO}} \quad (1)$$

The negative value of E_{LUMO} is similarly related to the electron affinity (A) [28] such as

shown in equation 2:

$$A = -E_{\text{LUMO}} \quad (2)$$

Energy gap (ΔE) is estimated by using E_{HOMO} and E_{LUMO} :

$$\Delta E = E_{\text{LUMO}} - E_{\text{HOMO}} \quad (3)$$

Electronegativity (χ) is estimated using following the equation 4 from I and A [29, 30]:

$$\chi = \left(\frac{I + A}{2} \right) \quad (4)$$

The chemical hardness (η) measures the resistance of an atom to a charge transfer [29], it's estimated by using the equation 5 from I and A [30] or E_{HOMO} and E_{LUMO} :

$$\eta = \left(\frac{I - A}{2} \right) = \left(\frac{E_{\text{LUMO}} - E_{\text{HOMO}}}{2} \right) \quad (5)$$

The electron polarizability is called chemical softness (σ), describes the capacity of an atom or group of atoms to receive electrons [29] and it is estimated from chemical hardness or E_{HOMO} and E_{LUMO} by using the equation 6:

$$\sigma = \frac{1}{\eta} \cong - \left(\frac{2}{E_{\text{HOMO}} - E_{\text{LUMO}}} \right) \quad (6)$$

The chemical potential (μ) and electronegativity (χ) can be calculated with the help of the following equations [21] from E_{HOMO} and E_{LUMO} :

$$\mu = -\chi \cong \left(\frac{E_{\text{HOMO}} + E_{\text{LUMO}}}{2} \right) \quad (7)$$

The global electrophilicity index (ω) is a useful reactivity descriptor that can be used to compare the electron-donating abilities of molecules [31]. A high value of electrophilicity describes a good electrophile while a small value of electrophilicity describes a good nucleophile [32]. ω is estimated by using the electronegativity and chemical hardness parameters through the equation:

$$\omega = \frac{\chi^2}{2\eta} \quad (8)$$

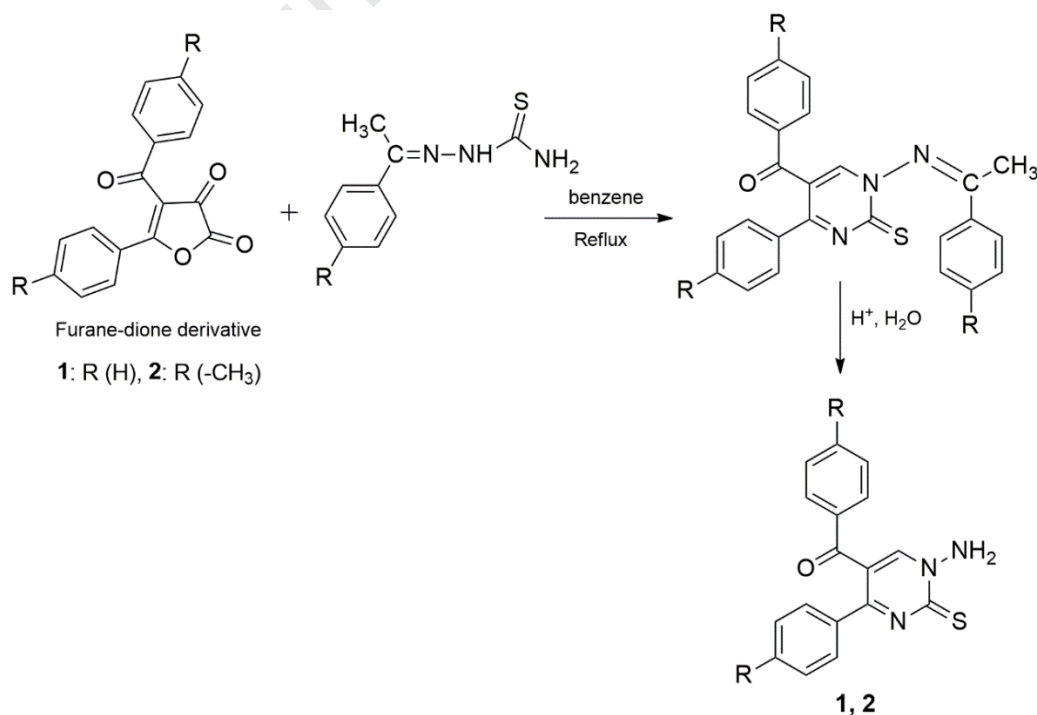
2.3. Cytotoxic activity study

Cytotoxic activity studies were conducted according to published literature procedure [33-35]. MDA-MB-231 and HepG2 were cultured in DMEM medium supplemented with 1% Glutamax and 10% FBS. The cancerous cells were seeded into sterile 96-well plates at a density of 4×10^3 cells/well. These plates were placed in an incubator. After 24 h incubation time, seeding cells were exposed to synthesized drug candidates **3** and **4** at six different concentrations following 5, 10, 20, 50, 100 and 200 μM . Then, plates were again incubated for 24 h (for HepG2) or 48 h (for MDA-MB-231). In the following step, MTT stock solution (50 μL , 5 mg/mL) was put to each well and was incubated for 3 h. After the time completed, medium was replaced with 200 μL of DMSO. Using Promega reader device, the absorbance values were measured at 560 nm. IC_{50} values were calculated with GraphPad Prism 7 software program.

3. Results and Discussion

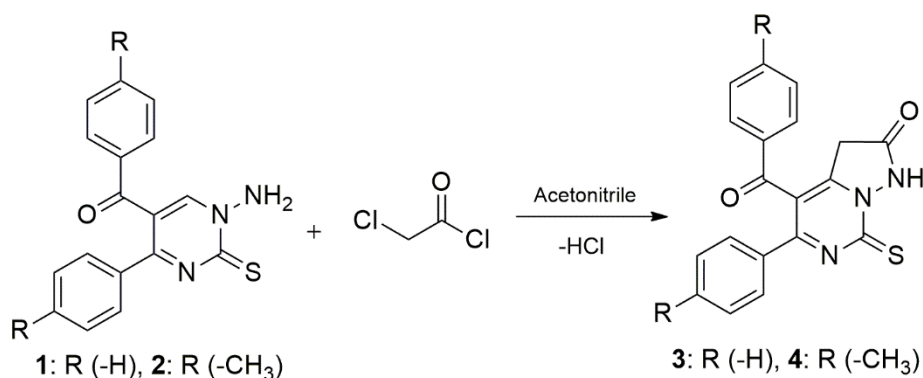
3.1. Structural analysis

The 1-amino-2-thioxo-1,2-dihydropyrimidin derivatives **1** and **2** were synthesized according to the reported literature procedure [12] as shown in **Scheme 1** [19].



Scheme 1. Synthesis of 1-amino-2-thioxo-1,2-dihydropyrimidin derivatives (**1** and **2**).

Two new 7-thioxopyrazolo[1,5-f]pyrimidin-2(1*H*,3*H*,7*H*)-one derivatives (**3** and **4**) were prepared in excellent yields (78 and 80%) from the reaction of chloroacetyl chloride with **1**, **2** compounds in the presence of a catalytic amount of sodium acetate (**Scheme 2**). The structures of the new compounds **3** and **4** were characterized using elemental analysis, ¹H NMR, ¹³C NMR and FT-IR spectroscopic techniques (for details see Experimental Section). The proposed mechanism for the formation of **3** and **4** is depicted in **Scheme 3**.



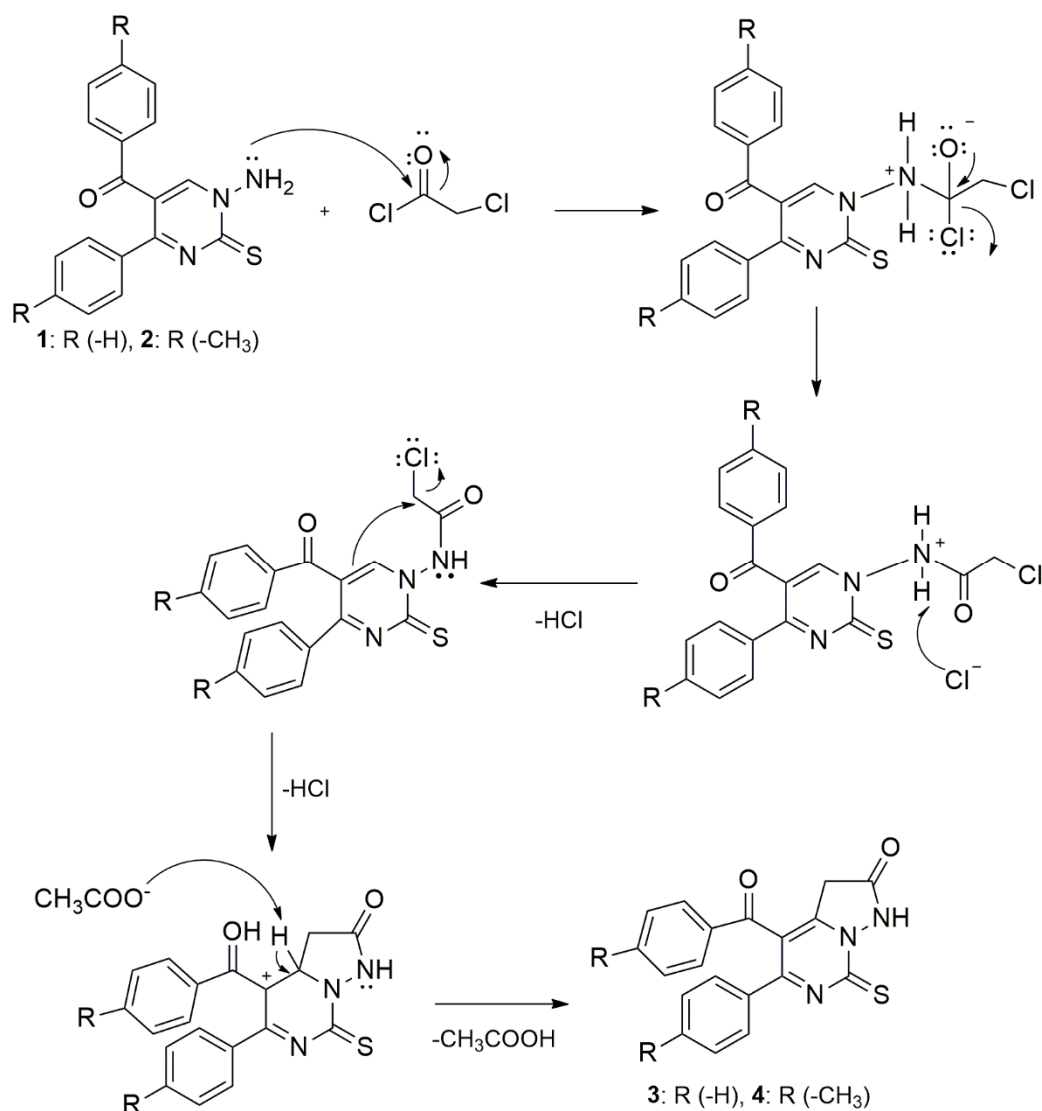
Scheme 2. Synthetic scheme for the compounds **3** and **4**.

Chloroacetyl chloride is active compound that is often used as a two-carbon building block reagent given its multi-functional properties [36]. The reaction is initiated by the nucleophilic attack of the nitrogen atoms of **1**, **2** directed to carbonyl's group of chloroacetyl chloride. At the first step, chloroacetamide derivatives occur by the nucleophilic acyl substitution of 1-amino-2-thioxo-1,2-dihydropyrimidin derivatives. At the last step, chloroacetamide derivatives go through a rearrangement to yield novel heterocyclic compounds **3**, **4** via intramolecular cyclization reaction takes place to give new five-membered part of compounds **3**, **4** called as a pyrazole ring.

Compound **3** was obtained in 78% yield by treating chloroacetyl chloride with **1** in acetonitrile at room temperature for 5 h. The structure of the compound **3** was confirmed by its analytical and spectral data. When the IR spectra of compounds **3**, **4** were compared with that of the compounds **1** and **2**, the absence of NH₂ around at 3350-3250 cm⁻¹ verify the structure of compounds **3** and **4**. NH- tensile vibrations of aromatic primary amines were observed at around 3350-3250 cm⁻¹ [19]. A characteristic stretching absorption band was obtained at 3060 cm⁻¹ for pyrimidine ring of compound **3**. In the IR spectrum of compound **3**,

the two C=O and C=S absorption bands were found (theo.) to be at 1650 (1696) (for C=O in benzoyl group), 1668 (1817) (for C=O in pyrazole ring) and 1274 (1327) (for C=S) cm^{-1} .

^1H NMR spectrum of compound **3** showed signals at δ 7.80-7.28 (8.81-7.45) ppm for aromatic protons. The peak at δ 8.53 (10.14) ppm represented the -NH. In the ^{13}C NMR spectrum of compound **3**, the peaks corresponding to δ 190.6 (201.6) and 26.5 (44.2) ppm indicated the presence of carbonyl (C=O) and methylene (CH_2) groups, respectively.



Scheme 3. Proposed mechanistic path for the synthesis of compounds (**3**, **4**).

The reaction of compound **2** with chloroacetyl chloride leads to form compound **4**. The IR spectrum of **4** exhibited stretching frequencies at 3066 (3206-3168) and 2964 (3114-3112) (for the aromatic C-H, aliphatic C-H), 1664 (1815) and 1644 (1637) cm^{-1} (for the two C=O groups). In addition, the presence of absorption band corresponding thiocarbonyl (C=S)

was observed as found (theo.) at 1271 (1328) cm^{-1} . Its ^1H NMR spectrum displayed four singlet signals at δ 8.43 (10.14), 3.60 (4.73-3.75), 2.42 and 2.33 (2.74-2.19) ppm due to NH, CH_2 and two CH_3 protons, respectively. Aromatic protons were observed in the region δ 7.72-7.14 (8.67-7.18) ppm as multiplet. ^{13}C NMR spectrum of **4** showed signals at δ 190.3 (201.0) ppm which was assigned to ph-C=O . The signals for methylene and methyl carbons were observed at δ 26.6 (44.2), 21.9 (24.1) and 21.6 (24.0) ppm. The other carbons were observed in the region of δ 166.7 (178.3)-128.1 (122.4) ppm.

3.2. Absorption spectroscopy study

The absorption spectra of the compounds were recorded in DMSO and are shown in **Fig. 1**.

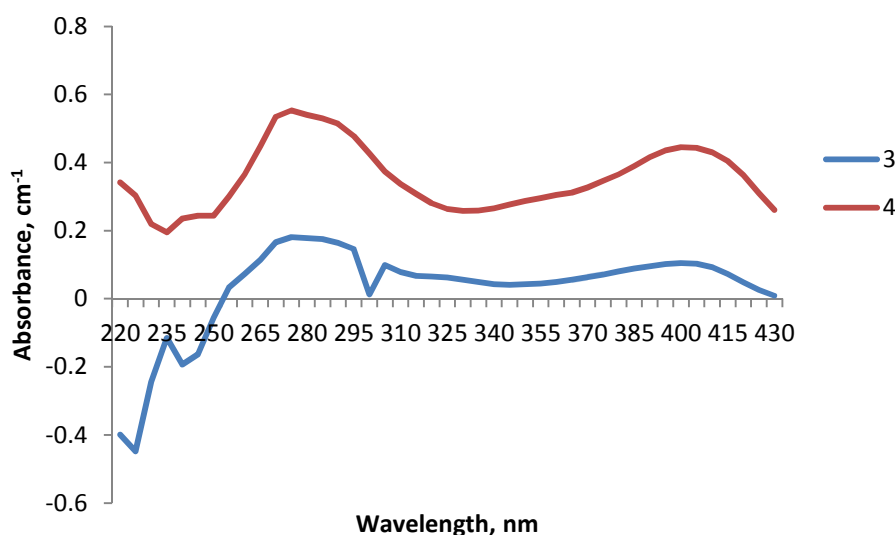


Fig. 1. UV-Vis absorbance spectra of compounds.

The maximum UV-Vis absorption spectra result for compounds **3** and **4** were screened from 200 to 800 nm. The absorption spectra were computed using the TDDFT method in combination with the same functional, basis set in gas phase. The calculated maximum absorption wavelengths (λ_{max}), and electronic transitions are shown in **Table 1**. The highest absorption values were obtained at 275 and 400 nm for compound **3**, and 280 and 400 nm for compound **4** as experimental, and the highest absorption values were calculated at 290 and 386 nm for compound **3**, and at 294 and 383 nm for compound **4**. It was found that the intense

band at 290 nm can be considered HOMO-3 \rightarrow LUMO, HOMO-3 \rightarrow LUMO+1, HOMO-2 \rightarrow LUMO, HOMO-1 \rightarrow LUMO+2, HOMO \rightarrow LUMO+2 translations for compound **3** and the translations at 294 were composed of HOMO-1 \rightarrow LUMO, HOMO \rightarrow LUMO, HOMO \rightarrow LUMO+1, HOMO \rightarrow LUMO+2 for compound **4**.

Table 1

Theoretical UV-Vis absorbance spectra of compounds.

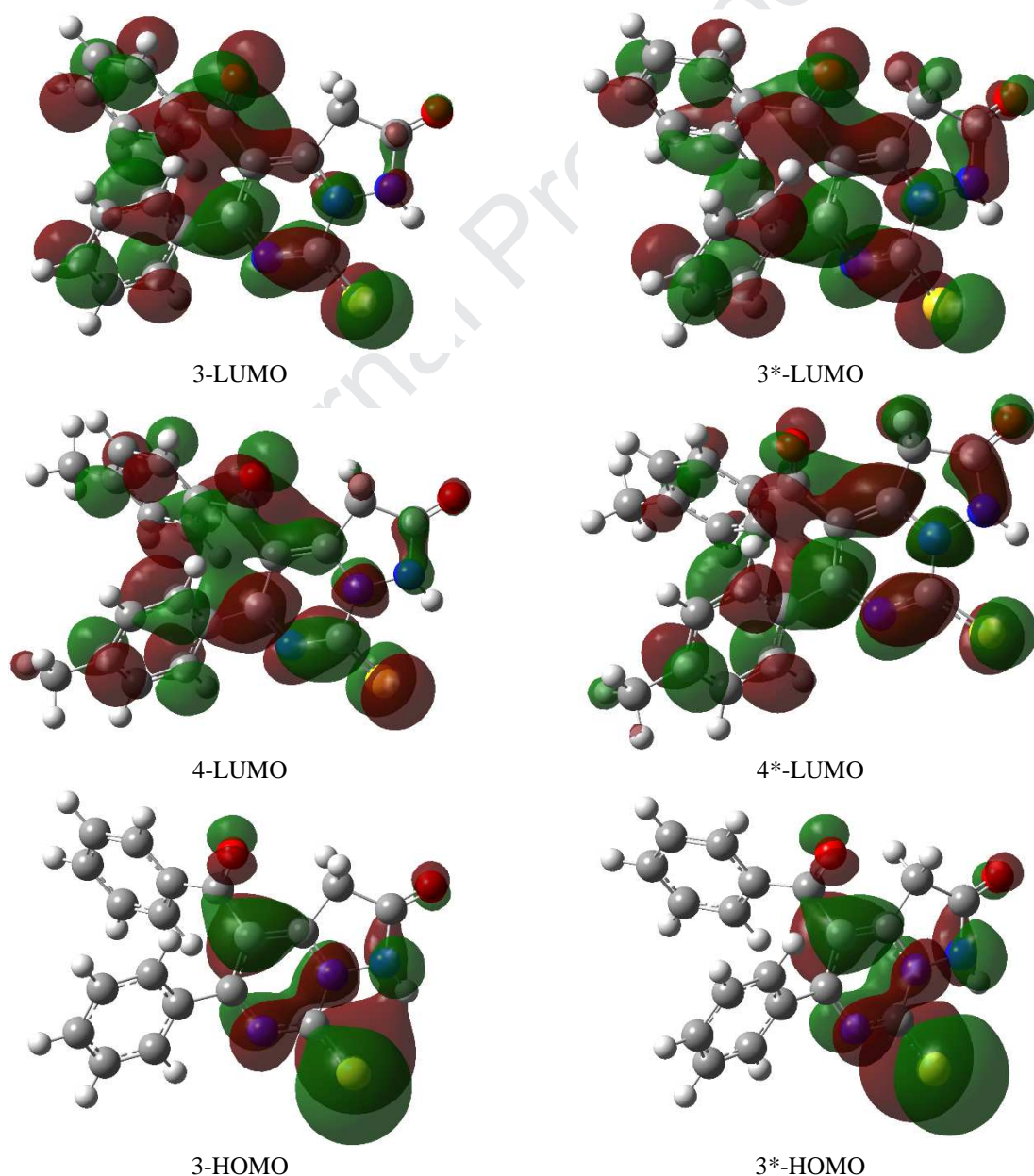
Compounds	Electronic Transitions	λ_{\max}	Electronic Transitions	λ_{\max}
3	HOMO-3 \rightarrow LUMO	290	HOMO-1 \rightarrow LUMO	386
	HOMO-3 \rightarrow LUMO+1		HOMO \rightarrow LUMO	
	HOMO-2 \rightarrow LUMO		HOMO \rightarrow LUMO+1	
	HOMO-1 \rightarrow LUMO+2		HOMO \rightarrow LUMO+2	
	HOMO \rightarrow LUMO+2			
4	HOMO-5 \rightarrow LUMO	294	HOMO-1 \rightarrow LUMO	383
	HOMO-4 \rightarrow LUMO		HOMO \rightarrow LUMO	
	HOMO-3 \rightarrow LUMO+1		HOMO \rightarrow LUMO+1	
	HOMO-1 \rightarrow LUMO+2		HOMO \rightarrow LUMO+2	

3.3. Molecular structure

The E_{HOMO} , E_{LUMO} , ΔE , I , η , σ , χ , etc. values were calculated for **3** and **4** with the DFT/B3LYP/6-311++G(2d,2p) method for gas and ethanol phase of neutral molecules, as shown in **Figs 2-5**, and **Tables 2** and **3**.

The HOMO and LUMO are known as frontier orbitals, and these molecules play important role in the determination of their molecular reactivity or stability. Some researchers mention that frontier molecular orbital (FMO) theory is useful in predicting interaction center of molecule [37]. The FMOs of the molecules **3** and **4** are given in **Fig. 2**. It could be easily found that the HOMO distributions of **3** and **4** compounds are mainly located around of pyrimidine ring, amine group and sulphur for gas and solvent phase of neutral molecules. **Fig.**

2 shows that the HOMO distributions for gas and solvent phase of the compounds **3** and **4** are approximately in the same regions. The electron-rich regions of the molecule can be said to be more active. The presence of nitrogen, oxygen and sulphur atoms on these molecules are cause to be strong activity. This figure shows that there is much more electron density in nitrogen, oxygen and sulphur atoms of **3** and **4** for both phases. The results show that the molecules are easier to interact with these bound atoms. It can be seen from **Fig. 2** that the LUMO distributions of the molecules for gas and solvent phase are similar for molecules **3** and **4**. The LUMO distributions of **3** and **4** are mainly located around of all molecules. According to the FMO, the chemical reactivity of molecule is a function of interaction between HOMO and LUMO levels of the reacting species.



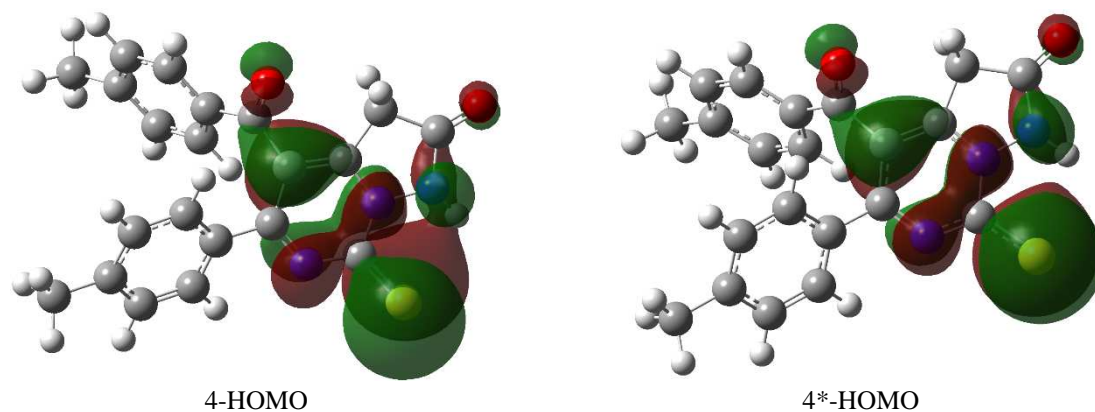


Fig. 2. Frontier MOs (HOMOs, LUMOs) molecules by using DFT/B3LYP/6-311++G(2d,2p) basic set for gas and ethanol (*) phase.

E_{HOMO} and E_{LUMO} are associated with electron donating and electron accepting ability of a molecule, respectively. High E_{HOMO} is essential for reaction with nucleophiles of molecule while low E_{LUMO} is essential for reaction with electrophiles [38]. E_{HOMO} values were found as -6.34, -6.24 eV for gas phase, and -6.50, -6.46 eV for solvent phase for **3** and **4**, respectively (**Fig. 3**). According to these results, molecule **3** was found to be more reactive than the other molecule **4** for gas and solvent phase. E_{HOMO} values in molecule **3** is higher than the other molecule. This is due to the methyl group attached to the phenyl ring. The methyl group is an electron donor group.

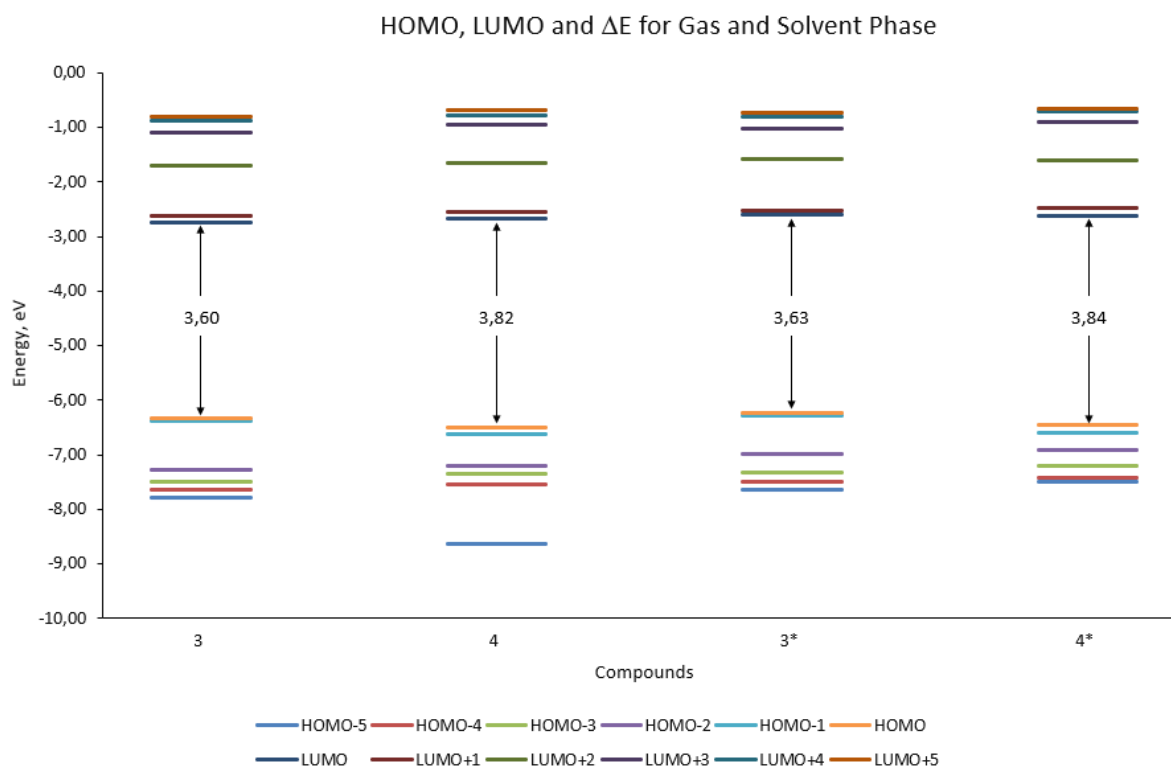


Fig. 3. Calculated HOMO, LUMO and energy gap (ΔE) parameters for gas and solvent (*: ethanol) phase of neutral molecules using B3LYP/6-311++G(2d,2p) method.

HOMO-LUMO energy gap (ΔE , see eq. 3), chemical hardness and softness are closely related to chemical properties [39, 40]. The physical properties of the compounds are strongly dependent on ΔE values. The large ΔE indicates a high kinetic stability and also low molecular activity of the compound. Because it is more difficult for molecules with high ΔE values to be polarized. The compounds need more energy to excite but lower gaps of the energy are relatively easy to polarize and it reacts more efficiently than higher values of the energy gaps [41]. Pearson showed that hard molecules with a high ΔE values are more stable compared to soft molecules with a low ΔE values [42]. The smaller ΔE is often interpreted by a stronger activity and perhaps greater inhibition efficiency [43]. So, ΔE decreases, the reactivity of the molecule increases leading to a better inhibition efficiency and activity [40]. ΔE values were found as 3.60, 3.82 eV in gas phase and 3.63, 3.84 eV in solvent phase for **3** and **4**, respectively. ΔE values in the gas phase are lower than the solvent phase. Therefore, the gas phase is expected to be more active than solvent phase. This is due to the dielectric coefficient of the solvent. In this case, molecule **3** is found more active than molecule **4** for both phases due to the fact that a low ΔE value is observed (**Fig. 3**).

The ionization potential (I) is one of the fundamental indicators of the chemical reactivity. High values of the ionization potential (Eq. 1) evidence the chemical inertness and strong stability, whereas small ionization potential denotes high activity of the atoms and molecules [44]. According to ionization potential values, order of activity can be written as: **4** (6.24 eV) < **3** (6.34 eV) for gas phase, and **4** (6.46 eV) < **3** (6.50 eV) for solvent phase (**Fig. 4**). As in ΔE values, in the gas phase I values are lower than the solvent phase for **3** and **4**. Molecule **4** is found more active than molecule **3** for gas and solvent phase. Because, molecule **4** has the lowest ionization potential value. It can be seen from the results that the stable for gas and water phase belongs to molecule **3** (**Fig. 4**).

Chemical hardness introduced in 1960s by Pearson is defined as the resistance towards electron cloud polarization or deformation of chemical species [38]. According to the Maximum Hardness Principle states; “a chemical system tends to arrange itself so as to achieve maximum hardness and chemical hardness can be considered as a measurement of stability”. The hardness (η) and softness (σ) are widely used in chemistry for explaining stability of compounds. According to Maximum Hardness Principle, chemical hardness is a measure of the stability of chemical species. The hardness is just half the energy gap between the E_{HOMO} and E_{LUMO} (see eq. 5). If a molecule has a large energy gap, it is called hard and otherwise is called soft [42]. The active compounds have a greater softness value. Softness (see eq. 6) is a measure of the polarizability and soft molecules give more easily electrons to an electron acceptor molecule or surface [21]. The calculated chemical hardness and softness values are given in **Fig. 4**. According to softness values, electron donating trend of studied chemical compounds may be written as **3** is more than **4** for gas and solvent phase. The softness values for gas phase were found as 0.55, 0.55 eV, and 0.52, 0.52 eV in solvent phase for molecules **3** and **4**, respectively.

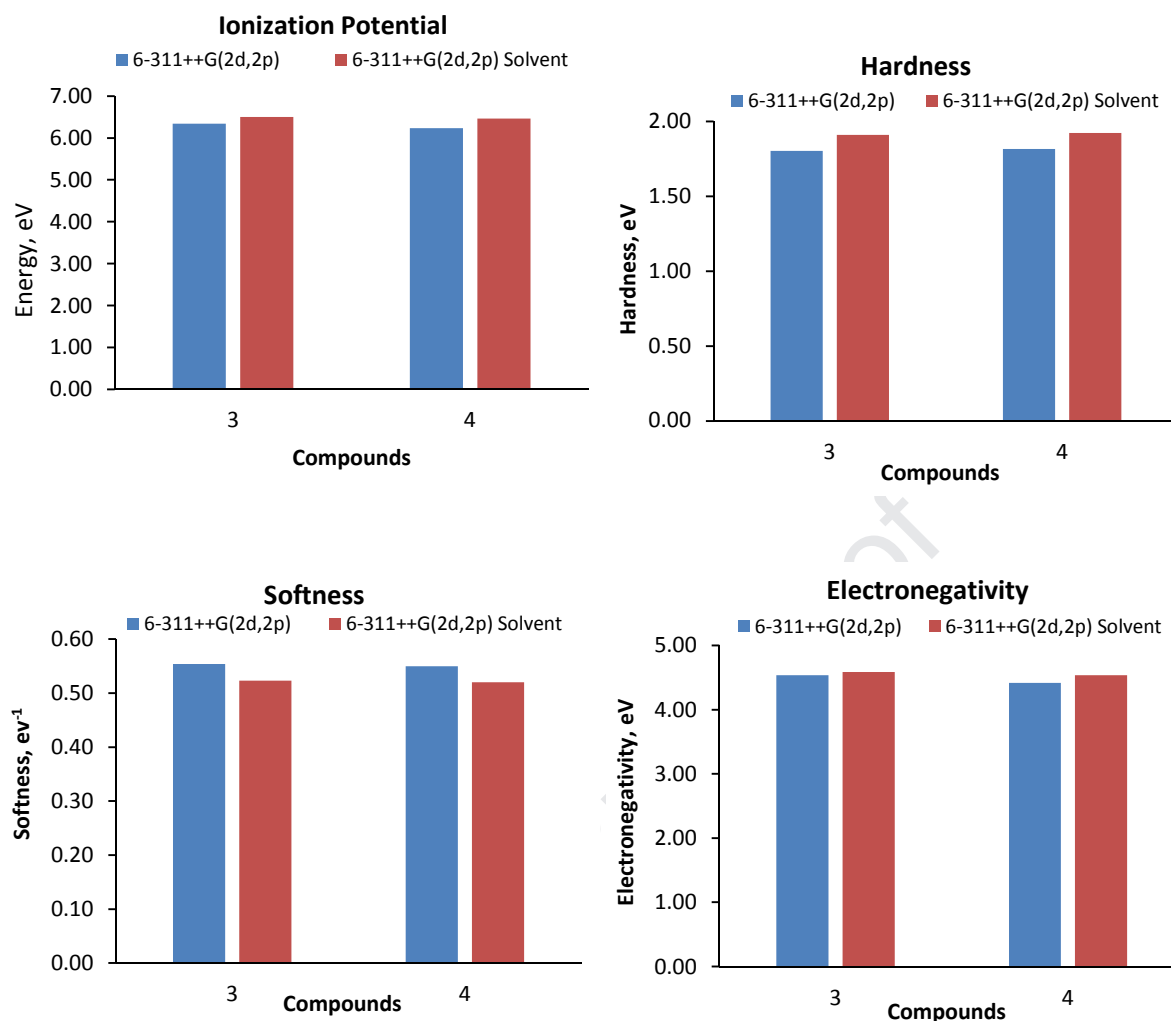


Fig. 4. Calculated some quantum chemical parameters for gas and solvent phase using B3LYP/6-311++G(2d,2p) method (solvent: ethanol).

The average values of the HOMO and LUMO energies have been defined as the chemical potential (μ). The negative value of the chemical potential was known as the electronegativity (χ) (see eq. 4). Chemical potential, electronegativity and hardness are descriptors for the predictions about chemical properties of the molecules [45]. The electronegativity also indicates the propensity of an inhibitor molecule to accept electrons or electron density. Electronegativity that represents the power to attract the electrons of chemical species is a useful quantity in the prediction of activity of the molecules [21]. In generally, a molecule with lower electronegativity is associated with higher electron donating tendency and therefore exhibited higher activity as compare to a molecular with higher value of electronegativity. The χ values were found as 4.54, 4.42 eV for gas phase and 4.59, 4.54

eV for solvent phase of **3** and **4**, respectively. According to the electronegativity values, molecule **3** was found to be more active than molecule **4** for both phases (see **Fig. 4**).

The dipole moment (DM) is another indicator of activity of chemical compounds. Although some authors reported that there is no remarkable relationship between dipole moment and inhibition efficiency and some authors showed that activity increases with the increasing of the dipole moment [46-48]. In some studies, authors supported that increasing value of dipole moment facilitates the electron transport process [47, 48]. For instance, DM values found are 6.99, 8.25 Debye in gas phase and 9.83, 11.46 Debye in solvent phase for **3** and **4**, respectively (**Table 2**). According to DM results, molecule **4** was found to be more active than compound **3** for gas and solvent phase.

Table 2

The calculated some quantum chemical parameters for gas and solvent phase of the neutral compounds using B3LYP/6-311++G(2d,2p) method.

Molecule	μ , eV	DM, Debye	MV, cm ³ /mol	TMAC, e	ω , eV
3	-4.54	6.99	208.86	-4.38	5.70
4	-4.42	8.25	266.72	-5.41	5.37
3*	-4.59	9.83	267.98	-4.94	5.51
4*	-4.54	11.46	268.00	-5.85	5.35

*Solvent phase: ethanol

The total of negative Mulliken atomic charges (TMAC) can be seen from **Table 2**. The TMAC values have been found as: -4.38 eV (for **3**), -5.41 eV (for **4**) in gas phase and -4.94 eV (for **3**), -5.85 eV (for **4**) in solvent phase. According to DM results, compound **4** was found as active molecule for both phases. The negative charge densities have been shown to increase on active molecules. The results of other calculations: global electrophilicity index (ω) and MV can be seen in **Table 2**.

DFT study can be used to better understand the molecular behaviour and structural conformation of the compounds. DFT approach helps to study the electrostatic potential (ESP) distribution of the compound more precisely [41]. Molecular Electrostatic Potential (MEP) is used to describe the electrostatic interaction between a molecule and an atom. ESP is indicating the electrophilic and nucleophilic nature of the molecules, and its essential tools to study the reactivity nature of the compounds. MEP maps at the surface are represented by

different colours. The blue colour in the ESP graphs, represents the maximum amount of the positive region where the nucleophilic reaction takes place and reddish region represented the negative region where the electrophilic reaction takes place [41], and green colour represents zero potential. ESP surfaces of investigation compounds are shown in **Fig. 5**.

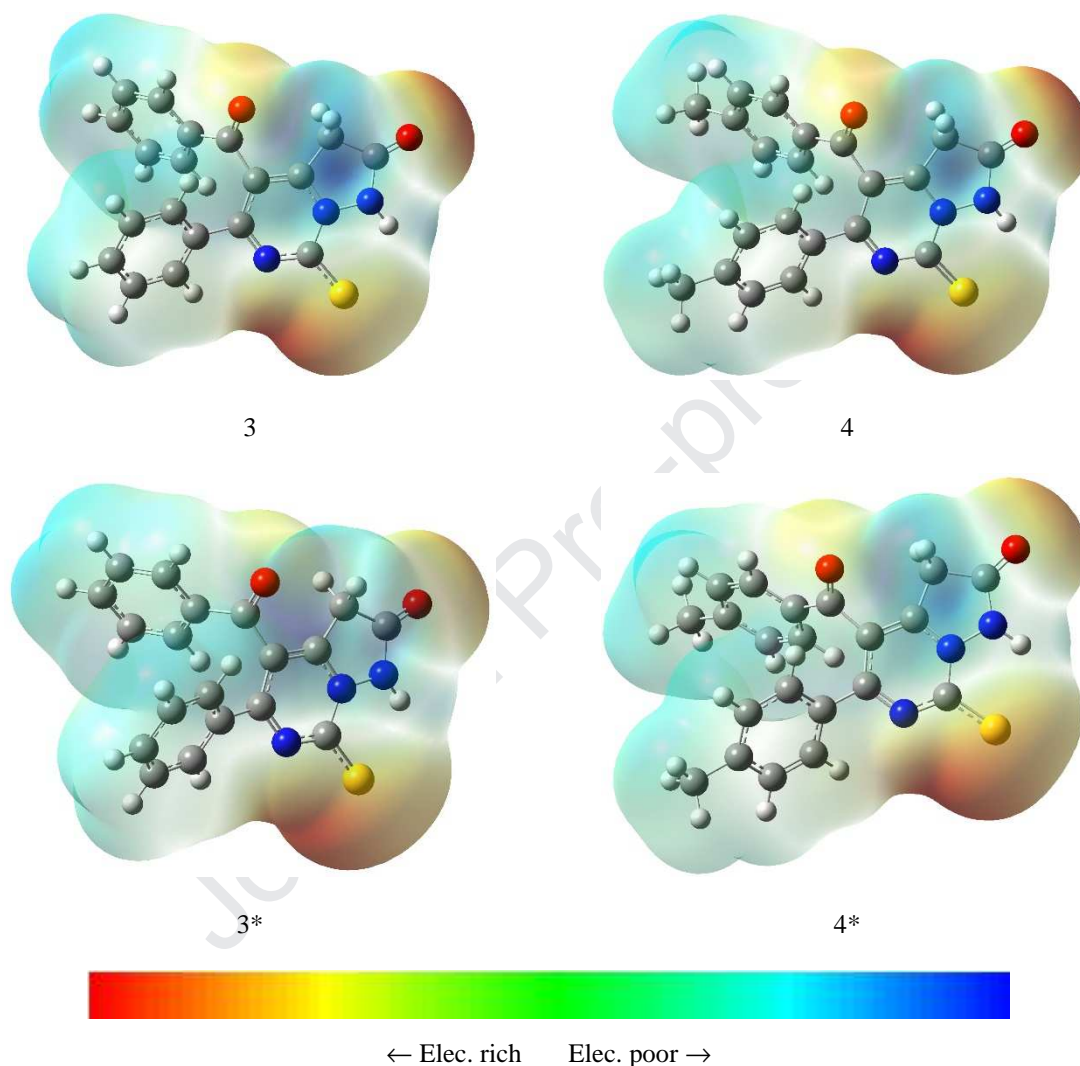


Fig. 5. Molecular electrostatic potential (MEP) surface of molecules by using DFT/B3LYP/6-311++G(2d,2p) basic set for gas and ethanol (*) phase.

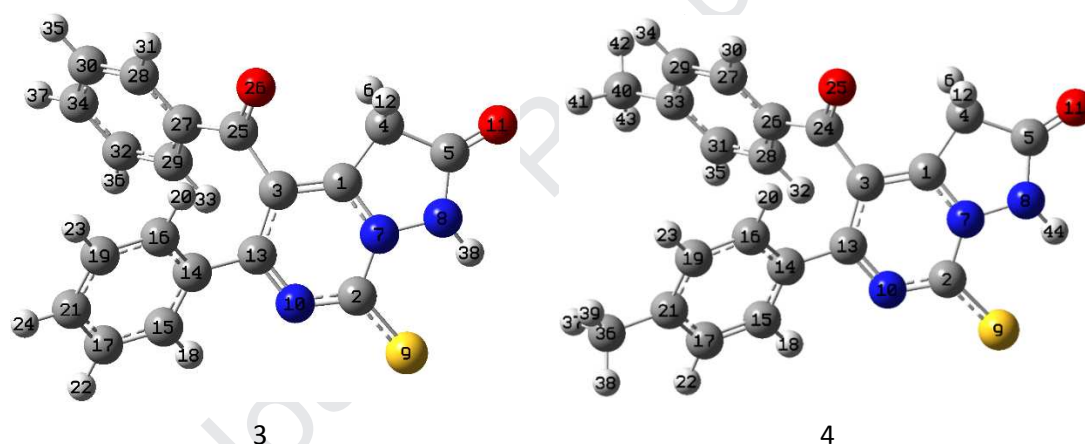
Fig. 5 shows that the electron density increases around the sulphur and oxygen atoms with the negative electrostatic potential values of the molecules for gas and solvent phase. Especially, most of the electrophilic reactions takes place of sulphur (9S), carbonyl oxygen (11O) of the pyrimidine ring and O25/26O oxygen atoms for both phase of compounds **3** and **4**, and the red coloured region in **Fig. 5** shows that the maximum electronegativity (the numbers of sulphur and oxygen atoms can be seen from the figure in **Table 3**). This result

indicates that these atoms will enter the electrophilic reactions more easily. On the other hand, it can be seen that the electron density decreases around 7N atom with the positive electrostatic potential values of the compounds.

In such studies, electronic charge analysis for atoms in the molecules is important because the binding capability of a molecule depends also on electronic charge on heteroatoms of the molecule. The binding facilitates as negative charge on heteroatom increases [49]. In this study, we used Mulliken population analysis to calculate the atomic charges. The Mulliken atomic charges on sulphur, nitrogen and oxygen of compounds **3** and **4** for non-protonated gas and solvent phases are given in **Table 3**.

Table 3

Calculated Mulliken atomic charges (e) on sulphur, nitrogen and oxygen atoms of compounds **3** and **4** by using B3LYP/6-311++G(2d,2p) basic set.



Atoms	3	4	3*	4*
7N	0.400	0.400	0.449	0.453
8N	-0.449	-0.459	-0.452	-0.461
9S	-0.656	-0.672	-0.774	-0.791
10N	-0.101	-0.091	-0.170	-0.168
11O	-0.450	-0.451	-0.530	-0.532
25O/26O	-0.405	-0.406	-0.448	-0.456

*Solvent phase: ethanol

In the ESP graphs (**Fig. 5**), the sulphur, nitrogen and oxygen atoms rich in electrons can be seen to have higher Mulliken charges. As can be seen from **Table 3**, the negative charge densities are more on 8N, 9S, O11 and 25O/26O number atoms. It is easier to bind a molecule from these atoms where the negative value is higher. It is seen that the negative charge values on these atoms are higher than **3** in molecule **4**. The Mulliken negative charges

values are generally lower in gas phase than in solvent phase. As a result, these atoms in the molecules cause to be strong interaction. This binding is expected to be stronger in molecule **4**.

3.4. Cytotoxic activity studies of compounds

Synthesized compounds **3** and **4** were screened towards MDA-MB-231 and HepG2 cell lines for 24/48 h. The IC₅₀ values calculated are given in **Table 4**.

Table 4

IC₅₀ results for synthesized compounds against MDA-MB-231 and HepG2 cell lines.

Compounds	IC ₅₀ , μ M	
	HepG2	MDA-MB-231
3	215.0	152.30
4	167.9	56.86
Cisplatin	139.1	N.T.*

N.T.* Not tested

When compounds (**3** and **4**) and positive control drug were screened in HepG2 cell line for 24 h, IC₅₀ values were obtained as >200, 167.9 and 139.1 μ M for **3**, **4** and cisplatin, respectively. In here, we saw the significance of the structure activity relationship. Because, when -CH₃ was chosen instead of -H as -R group, higher cytotoxic activity result was obtained in liver cell line. Furthermore, compound **4** containing -CH₃ group showed a value close to the IC₅₀ result of cisplatin, a well known clinical drug, in this cell line. According to E_{HOMO}, I, DM and TMAC results, molecule **4** was found to be more active than molecule **3**. This result also appears to be consistent with experimental cytotoxic activity values.

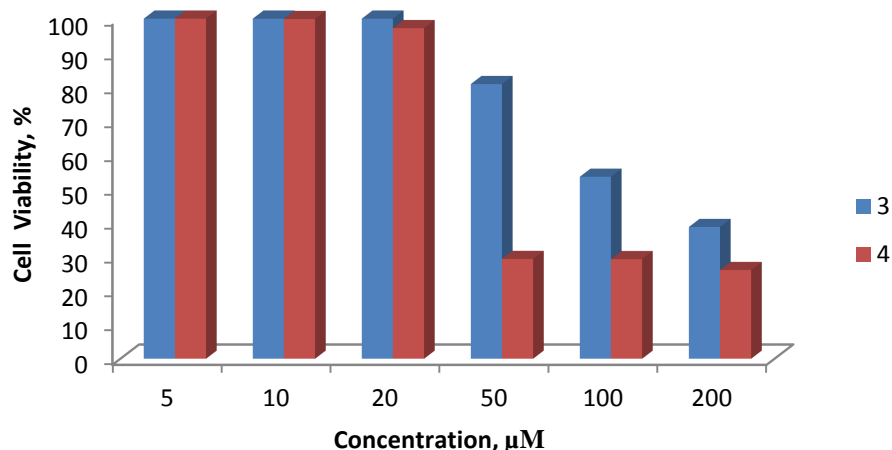


Fig. 6. Cell viability ratios of MDA-MB-231 depending on concentrations of molecules **3** and **4**.

Compounds **3** and **4** were also tested in MDA-MB-231 cell line for 48 h. It was found that they had activity in the breast cancerous cell line with following IC_{50} values; 152.30 and 56.86 μM for **3** and **4**, respectively. Compound **4** has a more toxic effect on MDA-MB-231 than **3**, too. Cell viability rates varied depending on the concentrations of the compounds tested. Cell viability at low concentrations is close to 100%, but it is seen from the figures 6 and 7 that this ratio decreases when high concentrations are reached.

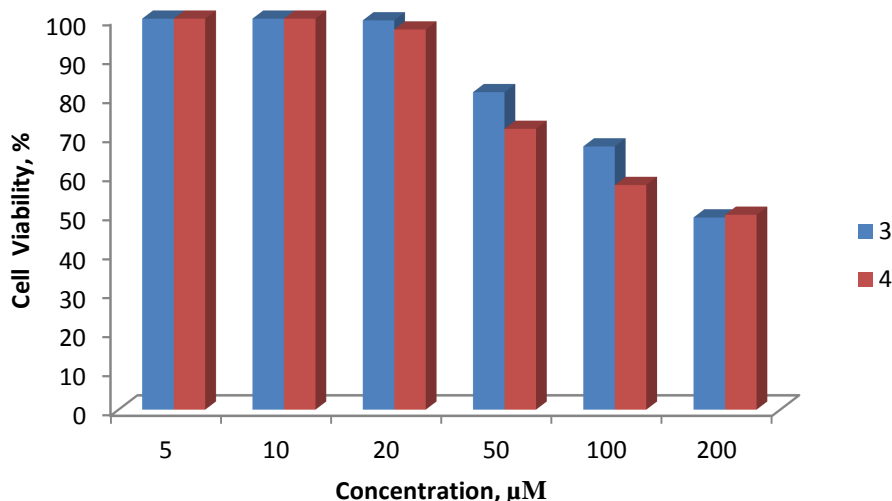


Fig. 7. Cell viability ratios of HepG2 depending on concentrations of molecules **3** and **4**.

4. Conclusions

As conclusion, starting from 1-amino-2-thioxo-1,2-dihydropyrimidin derivatives **1** and **2**, we successfully synthesized two derivatives of 7-thioxopyrazolo[1,5-f]pyrimidin-2(1*H*,3*H*,7*H*)-one (**3**, **4**). Both experimental techniques and theoretical methods were used to determine the structural and spectroscopic properties of these newly synthesized compounds. The structures of compounds were completely verified using ^1H NMR, ^{13}C NMR, elemental analysis and IR. For example; characteristic proton signal of N-H was obtained as singlet at δ 8.53 and 8.43 ppm for **3** and **4**, respectively. Methyl protons ($-\text{CH}_3$) at para positions of phenyl and benzoyl groups in the structure of compound **4** were seen as singlet signal at δ 2.42 and 2.33 ppm. In the ^{13}C NMR spectra, carbonyl ($\text{C}=\text{O}$) signals belongs to benzoyl group were found to be resonated in the lowest area and obtained at 190.6 and 190.3 ppm for **3** and **4**, respectively. The quantum chemical parameters of **3** and **4** were calculated and discussed. According to E_{HOMO} , I, DM and TMAC results, the molecule **4** was found to be more active than the molecule **3** for the gas and solvent phases of neutral compounds. Furthermore, the cytotoxic activity studies of these molecules were done and molecule **4** was found to be more active than **3** against two cancerous cell lines. It can be said that the cytotoxic activity results are consistent with the quantum chemical results.

Conflict of interest

The authors have no conflict of interest to declare.

Supporting Information

Supplementary data can be found in the online version.

Acknowledgements

This study was financially supported by Erciyes University Research Fund (FBY-12-4048) and the computers allocated by Erciyes University data center were used for quantum chemical calculations.

References

- [1] J. Zhang, J.F. Peng, Y.B. Bai, P. Wang, T. Wang, J.M. Gao, Z.T. Zhang, Synthesis of pyrazolo[1,5-a]pyrimidine derivatives and their antifungal activities against phytopathogenic fungi in vitro, *Mol. Divers.* 20 (2016) 887-896.

- [2] H. Zhang, R.F. Schinazi., C.K. Chu, Synthesis of neplanocin F analogues as potential antiviral agents, *Bioorg. Med. Chem.* 14 (2006) 8314-8322.
- [3] H. Shao, S. Shi, S. Huang, A.J. Hole, A.Y. Abbas, S. Baumli, X. Liu, F. Lam, D.W. Foley, P.M. Fischer, M. Noble, J.A. Endicott, C. Pepper, S. Wang, Substituted 4-(thiazol-5-yl)-2-(phenylamino)pyrimidines are highly active CDK9 inhibitors: synthesis, X-ray crystal structures, structure-activity relationship, and anticancer activities, *J. Med. Chem.* 56 (2013) 640-659.
- [4] P.F. Tuby, T.W. Hudyma, M. Brown, J.M. Essery, R.A. Partyka, Preparation and antiinflammatory properties of some 5-(2-anilinophenyl)tetrazoles, *J. Med. Chem.* 11 (1968) 111-117.
- [5] S.A. Rahaman, Y.R. Pasad, P. Kumar, B. Kumar, Synthesis and anti-histaminic activity of some novel pyrimidines, *Saudi Pharm. J.* 17 (2009) 255-258.
- [6] G. Marriapan, B.P. Saha, L. Sutharson, A. Haldar, Synthesis and bioactivity evaluation of pyrazolone derivatives, *Indian. J. Chem.* 49B (2010) 1671-1674.
- [7] N. Uramaru, H. Shigematsu, A. Toda, R. Eyanagi, S. Kitamura, Shigeru Ohta, Design, synthesis, and pharmacological activity of nonallergenic pyrazolone-type antipyretic analgesics, *J. Med. Chem.* 53 (2010) 8727-8733.
- [8] J. Choi, Y. Park, H.S. Lee, Y. Yang, S. Yoon, 1,3-Diphenyl-1H-pyrazole derivatives as a new series of potent PPAR γ partial agonists, *Bioorg. Med. Chem.* 18 (2010) 8315-8323.
- [9] T. Novinson, B. Bhooshan, T. Okabe, G.R. Revankar, H.R. Wilson, R.K. Robins, K. Senga, Novel heterocyclic nitrofurfural hydrazones, *In vivo* nosomal activity, *J. Med. Chem.* 19 (1976) 512-516.
- [10] K. Senga, T. Novinson, H.R. Wilson, R.K. Robins, Synthesis and antischistosomal activity of certain pyrazolo[1,5-*a*]pyrimidines, *J. Med. Chem.* 24 (1981) 610-613.
- [11] M. Suzuki, H. Iwasaki, Y. Fujikawa, M. Sakashita, M. Kitahara, R. Sakoda, Synthesis and biological evaluations of condensed pyridine and condensed pyrimidine-based HMG-CoA reductase inhibitors, *Bioorg. Med. Chem. Lett.* 11 (2001) 1285-1288.
- [12] C. Almansa, A.F. Arriba, F.L. Cavalcanti, L.A. Gomez, A. Miralles, M. Merlos, J.G. Rafanell, J. Forn, Synthesis and SAR of a new series of COX-2-selective inhibitors: pyrazolo[1,5-*a*]pyrimidines, *J. Med. Chem.* 44 (2001) 350-361.
- [13] Z. Önal, B. Altural, Reactions of 1-Amino-5-benzoyl-4-phenyl-1H-pyrimidine-2-thione with various carboxylic anhydrides, *Asian J. Chem.* 18 (2006) 1061-1064.

- [14] Z. Önal, B. Altural, Reactions of N-Aminopyrimidine derivatives, with 1,3-dicarbonyl compounds, Turk. J. Chem. 23 (1999) 401-405.
- [15] S.R. Gondi, D.Y. Son, Synthesis *N,N'*-bis(2-thiazolinyl)-, *N,N'*-bis(2-thiazolyl)-, and *N,N'*-bis(2-pyrimidinyl)-benzene dicarboxamide, Synth. Commun. 34 (2004) 3061-3072.
- [16] Z. Çimen, S. Akkoç, Z. Kökbudak, Reactions of amino pyrimidine derivatives with chloroacetyl and isophthaloyl chlorides, Heteroatom Chem. 29 (2018) 1-6.
- [17] H.G. Aslan, S. Akkoç, Z. Kökbudak, L. Aydın, Synthesis, characterization and antimicrobial and catalytic activity of a new schiff base and its metal (II) complexes, J. Iran Chem. Soc. 14 (2017) 2263-2273.
- [18] M. Saracoglu, F. Kandemirli, A. Özalp, Z. Kökbudak, Synthesis and quantum chemical calculations of 2,4-dioxopentanoic acid derivatives-part II, Int. J. Sci. Eng. Inv. 6 (2017) 50-57.
- [19] Z. Önal, İ. Yıldırım, Reactions of 4-(4-methylbenzoyl)-5-(4-methylphenyl)-2,3-furandione with semi-thiosemi-carbazones, Heterocycl. Commun. 13 (2007) 113-120.
- [20] M.J. Frisch, G.W. Trucks, H.B. Schlegel, G.E. Scuseria, M.A. Robb, J.R. Cheeseman, G. Scalmani, V. Barone, B. Mennucci, G.A. Petersson, H. Nakatsuji, M. Caricato, X. Li, H.P. Hratchian, A.F. Izmaylov, J. Bloino, G. Zheng, J.L. Sonnenberg, M. Hada, M. Ehara, K. Toyota, R. Fukuda, J. Hasegawa, M. Ishida, T. Nakajima, Y. Honda, O. Kitao, H. Nakai, T. Vreven, J.A. Montgomery, Jr., J.E. Peralta, F. Ogliaro, M. Bearpark, J.J. Heyd, E. Brothers, K.N. Kudin, V.N. Staroverov, R. Kobayashi, J. Normand, K. Raghavachari, A. Rendell, J.C. Burant, S. S. Iyengar, J. Tomasi, M. Cossi, N. Rega, J.M. Millam, M. Klene, J.E. Knox, J.B. Cross, V. Bakken, C. Adamo, J. Jaramillo, R. Gomperts, R.E. Stratmann, O. Yazyev, A.J. Austin, R. Cammi, C. Pomelli, J.W. Ochterski, R.L. Martin, K. Morokuma, V.G. Zakrzewski, G.A. Voth, P. Salvador, J.J. Dannenberg, S. Dapprich, A.D. Daniels, O. Farkas, J.B. Foresman, J.V. Ortiz, J. Cioslowski, D.J. Fox, Gaussian 09, Revision A.02, Gaussian Inc., Wallingford CT, 2009.
- [21] S. Kaya, C. Kaya, L. Guo, F. Kandemirli, B. Tüzün, İ. Uğurlu, L.H. Madkour, M. Saracoglu, Quantum chemical and molecular dynamics simulation studies on inhibition performances of some thiazole and thiadiazole derivatives against corrosion of iron, J. Mol. Liq. 219 (2016) 497-504.

- [22] C.G. Zhan, P.S. Spencer, D.A. Dixon, Chromogenic and neurotoxic effects of an aliphatic γ -diketone: Computational insights into the molecular structures and mechanism, *J. Phy. Chem.* 108 (2004) 6098-6104.
- [23] M. Saracoglu, F. Kandemirli, A. Ozalp, Z. Kokbudak, Synthesis and Quantum Chemical Calculations of 2,4-dioxopentanoic Acid Derivatives-Part I, *Chem. Sci. Rev. Lett.* 6 (2017) 1-11.
- [24] M. Saraçoğlu, Z. Kökbudak, Z. Çimen, F. Kandemirli, Synthesis and DFT quantum chemical calculations of novel pyrazolo[1,5-c]pyrimidin-7(1*H*)-one derivatives, *J. Chem. Soc. Pak.* 41 (2019) 479-488.
- [25] M. Saraçoğlu, Z. Kökbudak, E. Yalçın, F. Kandemirli, Synthesis and DFT quantum chemical calculations of 2-oxopyrimidin-1(2*H*)-yl-thiourea and urea derivatives, *J. Chem. Soc. Pak.* 41 (2019) (in press).
- [26] K.F. Khaled, Studies of iron corrosion inhibition using chemical, electrochemical and computer simulation techniques, *Electrochim. Acta* 55 (2010) 6523-6532.
- [27] M.J. Dewar, W. Thiel, Ground states of molecules. 38. The MNDO method. Approximations and parameters, *J. Am. Chem. Soc.* 99 (1977) 4899-4907.
- [28] R.G. Pearson, Hard and soft acids and bases-the evolution of a chemical concept, *Coord. Chem. Rev.* 100 (1990) 403-425.
- [29] L. Pauling, *The Nature of the Chemical Bond*, Cornell University Press, Ithaca, New York, 1960.
- [30] R.G. Parr, R.G. Pearson, Absolute hardness: companion parameter to absolute electronegativity, *J. Am. Chem. Soc.* 105 (1983) 7512-7516.
- [31] P.K. Chattaraj, U. Sarkar, D.R. Roy, Electrophilicity index, *Chem. Rev.* 106 (2006) 2065-2091.
- [32] E.E. Ebenso, M.M. Kabanda, T. Arslan, M. Saracoglu, F. Kandemirli, L.C. Murulana, A.K. Singh, S.K. Shukla, B. Hammouti, K.F. Khaled, M.A. Quraishi, I.B. Obot, N.O. Edd, Quantum chemical investigations on quinoline derivatives as effective corrosion inhibitors for mild steel in acidic medium, *Int. J. Electrochem. Sci.* 7 (2012) 5643-5676.
- [33] S. Akkoç, V. Kayser, İ. Ö. İlhan, Synthesis and *in vitro* anticancer evaluation of some benzimidazolium salts, *J. Heterocycl. Chem.* (2019) (in press).
- [34] S. Akkoç, Derivatives of 1-(2-(Piperidin-1-yl)ethyl)-1*H*-benzo[*d*]imidazole: synthesis, characterization, determining of electronic properties and cytotoxicity studies, *ChemistrySelect.* 4 (2019) 4938-4943.

- [35] S. Akkoç, Antiproliferative activities of 2-hydroxyethyl substituted benzimidazolium salts and their palladium complexes against human cancerous cell lines, *Synth. Commun.* 49 (2019) 2903-2914.
- [36] G.A. Olah, S. Kobayashi, Aromatic substitution. XXIX. Friedel-Crafts acylation of benzene and toluene with substituted acyl halides. Effect of substituents and positional selectivity, *J. Am. Chem. Soc.* 93 (1971) 6964-6967.
- [37] K.F. Khaled, M.M. Al-Qahtani, The inhibitive effect of some tetrazole derivatives towards Al corrosion in acid solution: Chemical, electrochemical and theoretical studies, *Mater. Chem. Phys.* 113 (2009) 150-158.
- [38] A. Rauk, *Orbital Interaction Theory of Organic Chemistry*, Second ed., Wiley & Sons: New York, 2001.
- [39] N.O. Obi-Egbedi, I.B. Obot, M.I. El-Khaiary, Quantum chemical investigation and statistical analysis of the relationship between corrosion inhibition efficiency and molecular structure of xanthene and its derivatives on mild steel in sulphuric acid, *J. Mol. Struct.* 1002 (2011) 86-96.
- [40] I.B. Obot, N.O. Obi-Egbedi, E.E. Ebenso, A.S. Afolabi, E.E. Oguzie, Experimental, quantum chemical calculations, and molecular dynamic simulations insight into the corrosion inhibition properties of 2-(6-methylpyridin-2-yl)oxazolo[5,4-f][1,10]phenanthroline on mild steel, *Res. Chem. Intermed.* 39 (2013) 1927-1948.
- [41] D. Bhattacharjee, T.K. Devi, R. Dabrowski, A. Bhattacharjee, Polarizability order parameters and DFT calculations in the nematic phase of two bent-core liquid crystals and their correlation, *J. Mol. Liq.* 271 (2018) 239-252.
- [42] R.G. Pearson, The principle of maximum hardness, *Acc. Chem. Res.* 26 (1993) 250-255.
- [43] A.Y. Musa, A.A.H. Kadhum, A.B. Mohamad, A.A.B. Rohoma, H. Mesmari, Electrochemical and quantum chemical calculations on 4,4-dimethyloxazolidine-2-thione as inhibitor for mild steel corrosion in hydrochloric acid, *J. Mol. Struct.* 969 (2010) 233-237.
- [44] I.B. Obot, N.O. Obi-Egbedi, A.O. Eseola, Anticorrosion potential of 2-Mesityl-1H-imidazo[4,5-f][1,10]phenanthroline on mild steel in sulfuric acid solution: experimental and theoretical study, *Ind. Eng. Chem. Res.* 50 (2011) 2098-2110.
- [45] A. Özalp, Z. Kökbudak, M. Saraçoğlu, F. Kandemirli, İ.Ö. İlhan, C.D. Vurdu, Synthesis and theoretical study of the novel 2-oxopyrimidin-1(2*H*)-ylamides derivative, *Chem. Sci. Rev. Lett.* 4 (2015) 719-728.

- [46] G. Gao, C. Liang, Electrochemical and DFT studies of β -amino-alcohols as corrosion inhibitors for brass, *Electrochim. Acta.* 52 (2007) 4554-4559.
- [47] M. Sahin, G. Gece, F. Karci, S. Bilgic, Experimental and theoretical study of the effect of some heterocyclic compounds on the corrosion of low carbon steel in 3.5% NaCl medium, *J. Appl. Electrochem.* 38 (2008) 809-815.
- [48] M.A. Quraishi, R. Sardar, Hector bases a new class of heterocyclic corrosion inhibitors for mild steel in acid solutions, *J. Appl. Electrochem.* 33 (2003) 1163-1168.
- [49] J.N. Murrell, S.F. Kettle, J.M. Tedder, *The Chemical Bond*, Second ed., John Wiley & Sons, Chichester, UK, 1985.

Highlights:

- New compounds including pyrimidin nucleus were synthesized and characterized.
- Quantum-chemical calculations were made for finding molecular properties of these compounds.
- Cytotoxic activities of compounds were tested against HepG2 and MDA-MB-231 cell lines. Compound **4** gave higher anticancer activity than **3**.

Journal Pre-proof

Declaration of interests

The authors declare that they have no known competing financial interests or personal relationships that could have appeared to influence the work reported in this paper.

The authors declare the following financial interests/personal relationships which may be considered as potential competing interests: